

# Microfluidic spatial growth of vertically aligned ZnO nanostructures by soft lithography for antireflective patterning

Rupali S. Mehare · Rami Reddy Devarapalli ·  
Sandeep G. Yenchalwar · Manjusha V. Shelke

Received: 30 July 2012 / Accepted: 26 November 2012 / Published online: 7 December 2012  
© Springer-Verlag Berlin Heidelberg 2012

**Abstract** Hierarchical assemblies of nanostructured building blocks on conducting substrates are significant for construction of functional devices. Microfluidics is powerful but less exploited tool for spatial organization or growth of functionally sophisticated nanostructures with precise control. In this paper, we introduce a simple but unique strategy for the hydrothermal synthesis and patterned assembly of ZnO nanostructures within microchannels by soft lithography technique. Optical/antireflection properties of such hierarchically structured nanostructures are studied.

**Keywords** ZnO nanostructures · Microfluidics · Soft lithography · Micropatterning · Antireflective structures

## 1 Introduction

One dimensional inorganic nanostructures such as nanowires, tubes, rods, belts, etc. have drawn prime attention due to their significance in understanding fundamental physical concepts and constructing nanoscale electronic and optoelectronic devices (Duan et al. 2001; Huang et al. 2001; Yang et al. 2010). However, next generation devices will most likely require precisely engineered multiscale architectures of materials; hence, there is a rising demand to obtain functional materials with well defined and controllable structures (Qu et al. 2011). Fabrication of

functional nanostructures within well-defined micropatterns can synergize the advantages of both unique properties of nanomaterials and diverse applications of micropatterning of materials (Menard et al. 2007; Fan et al. 2006). Among functional nanomaterials vertically aligned ZnO nanostructures have a variety of applications in electronics as well as optoelectronic and electromechanical nanodevices, such as solar cells (Law et al. 2005), field emission devices (Wang et al. 2006a), UV lasers (Govender et al. 2002), light emitting diodes (Park and Yi 2004), piezo-nanogenerators (Wang and Song 2006) and nanosensors (Wang et al. 2004; Han et al. 2012). 1D ZnO nanostructures have been synthesized by several strategies as chemical or physical vapor deposition, molecular beam epitaxy (MBE), pulsed laser deposition or sputtering techniques (Djurisic et al. 2012). In comparison to these techniques wet chemical processes are low cost and scalable methods (Xu and Wang 2011). However, to realize the novel nanoscale device architectures the suitability of a fabrication technique for integration with higher level structures is as important as its capability of producing well-controlled nanostructures.

In an effort to integrate the ZnO nanostructures into a more regular form to enhance the performance of the nanodevices, a variety of techniques have been employed to fabricate patterned vertically aligned ZnO nanostructure arrays, including photolithography (Greyson et al. 2004), nanosphere lithography (Zeng et al. 2009), interference lithography (Kim et al. 2007), laser writing (Ong et al. 2012), electron beam lithography (EBL) (Ng et al. 2004) and nanoimprinting (Jung and Lee 2011). Mostly a seed layer is patterned with these techniques and then used to grow patterned arrays of ZnO nanostructures separately. These require clean rooms and expensive equipments and are low throughput techniques.

R. S. Mehare · R. R. Devarapalli · S. G. Yenchalwar ·  
M. V. Shelke (✉)  
Physical and Material's Chemistry Division,  
National Chemical Laboratory (CSIR-NCL),  
Dr. Homi Bhabha Road, Pune 411008, MH, India  
e-mail: shelkemanju@gmail.com; mv.shelke@ncl.res.in

Soft lithography is a low cost and experimentally convenient technology for patterning micro or nanoscale structures (Qin et al. 2010). Microcontact printing of a self assembled monolayer (SAM) has been employed in ZnO nanostructure patterning processes with chemically modified surfaces (Wang et al. 2007; Kang et al. 2011). The use of SAM patterning is clever but restricted by the limitations on compatible substrate materials. Microfluidics-based, surface-adherent synthesis offers a route towards simultaneous spatial patterning and growth of functional nanomaterials (Wang et al. 2006b; Thangawng et al. 2009; Dittrich et al. 2006). Crystals and nanoparticles of superior quality are synthesized in microchannels due to the excellent handling of small fluid volumes of nano- and even picolitres (Yen et al. 2005). However, microfluidic device is also a powerful tool to align inorganic nanostructures on substrate. There are only few reports on use of microfluidics to organize nanostructures with increased complexity/hierarchy. Indeed, in some cases, complex nanowire arrays are fabricated on substrates using fluid flows within the channel but nanostructures are synthesized ex-situ and then horizontally aligned within the channels using fluid flow (Kim et al. 2011; Cui and Lieber 2001; Kenis et al. 2000). In an effort to grow and pattern vertical arrays of nanostructures, a patterned seed template was fabricated by zinc acetate solution flowing through a microfluidic channel and then growth of vertical ZnO nanowires was realized from the seed using thermal chemical vapor deposition on a silicon substrate at high temperatures (Lee et al. 2006). An alternative, more simple strategy is to grow nanostructure arrays directly from Zinc metal substrates. The direct growth of ZnO arrays on zinc substrates was realized by the surface oxidation of zinc foil in solution at room temperature or under hydrothermal conditions (Wang et al. 2008). If Zn foil can be replaced with Zn plating layer, the growth of ZnO nanowire arrays could be extended to various substrates. By exploiting this concept we have successfully achieved micropatterned seedless vertical growth of functional ZnO nanostructures by means of soft microfluidic channels. The photoluminescence and antireflection characteristics of the hierarchically structured ZnO nanowire arrays are studied. Method reported here has the virtue of simplicity, cost efficiency and high throughput which can facilitate fabrication of complex device architectures.

## 2 Experimental

### 2.1 Fabrication of elastomeric patterned mold

Silicon masters with desired microchannels are fabricated using photolithography. In order to fabricate silicon

masters, Si wafers with native oxide layers were cleaned by sonication in acetone and ethanol for 15 min. They were subsequently rinsed with ethanol and dried with nitrogen flux. A photoresist (AZ 9260 Photoresist, Clarion corp.) was applied to the wafer, which was subsequently spun at 3,000 rpm for 30 s, and then the wafers were baked on a hot plate (110 °C) for 1 min 30 s. The resist was patterned by a mask aligner (SussMicroTech Lithography GmbH) and developed with AZ 300 MIF. To realize the patterns within the silicon for the master, ICP-RIE plasma etching system (SPTS Technologies, UK) was used. The Bosch process, consisting of pulsed SF<sub>6</sub>/C<sub>4</sub>F<sub>8</sub> deep reactive ion etching enables anisotropic etching of silicon through the photoresist mask. After the definition of the patterns within the bulk of the silicon wafer, the photoresist was removed by several baths in acetone and isopropyl alcohol. The patterns were then coated with a 60-nm thick C<sub>4</sub>F<sub>8</sub> fluoropolymer. Polydimethylsiloxane (PDMS) molds with micropatterns were fabricated with Sylgard 184 (Dow Corning) by molding against Si masters. These molds can be used repeatedly several times.

### 2.2 Microfluidic growth of patterned ZnO nanorod arrays

For the preparation of patterned ZnO nanostructure arrays, zinc substrates (zinc wafer cut into 1 × 1 cm<sup>2</sup>) were cleaned by sonication in ethanol, propanol and deionised water and dried in air. PDMS molds with micro patterns are kept in conformal contact with zinc substrate. This assembly was supported by Teflon thread tying to keep both substrate and PDMS mold in firm contact with each other forming microchannels throughout the reaction. This microchannel assembly is then placed in 100 ml of 15 % aqueous dimethylformamide solution (v/v). The reaction system was then maintained at a temperature of 85–90 °C for 12 h. After completion of reaction, microfluidic device is disassembled and Zn substrates with patterned ZnO nanostructures on it are removed, rinsed with absolute ethanol and dried in air for further characterization.

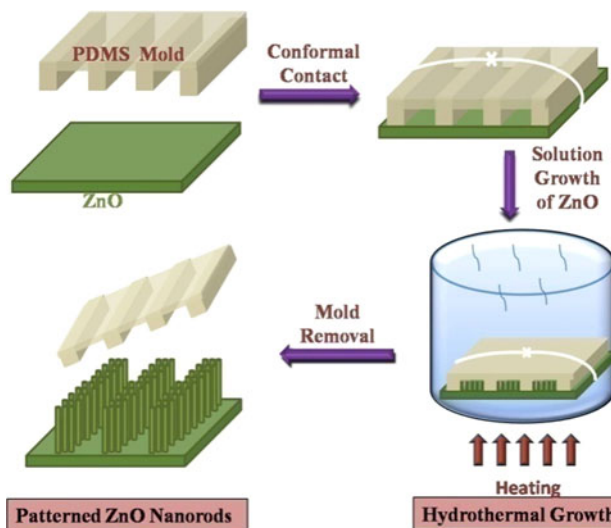
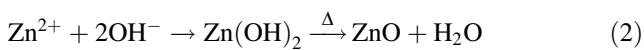
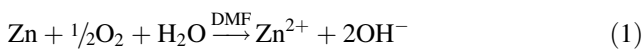
### 2.3 Characterization

The morphology of all the samples is examined by scanning electron microscopy (Quanta 200 3D, FEI). The X-ray diffraction measurements are carried out on a Philips PW 1830 instrument. HRTEM images and SAED patterns are obtained on a Tecnai F30 FEG machine operated at 300 kV. Raman analyses of all the samples were performed on an HR 800 Raman spectrometer (Jobin–Yvon, Horiba, France) using 632.8 nm green laser (NRS1500W).

The reflectance spectra of the ZnO nanorods are measured using Jasco UV–Vis spectrophotometer (V 570 UV–VIS–NIR). The photoluminescence properties are studied at room temperature on Fluorolog HoribaJobinYvon fluorescence spectrophotometer.

### 3 Results and discussion

Scheme 1 is the schematic representation of device assembly and subsequent microfluidic growth of ZnO nanostructures inside microchannels. Three walls of these microfluidic channels are composed of soft elastomeric mold, whereas the fourth wall or base of the microchannels acts as substrate on which and material by which ZnO nanostructures are grown. ZnO nanostructure arrays are grown by chemical oxidation of Zn wafer in 15 % dimethyl formamide (DMF) aqueous solution at 90 °C. Naturally dissolved oxygen in water oxidizes metallic zinc slowly due to the formation of passive oxide layer. The oxidation process of metallic zinc is accelerated by DMF. The mechanism for the formation of ZnO nanostructures is as below:

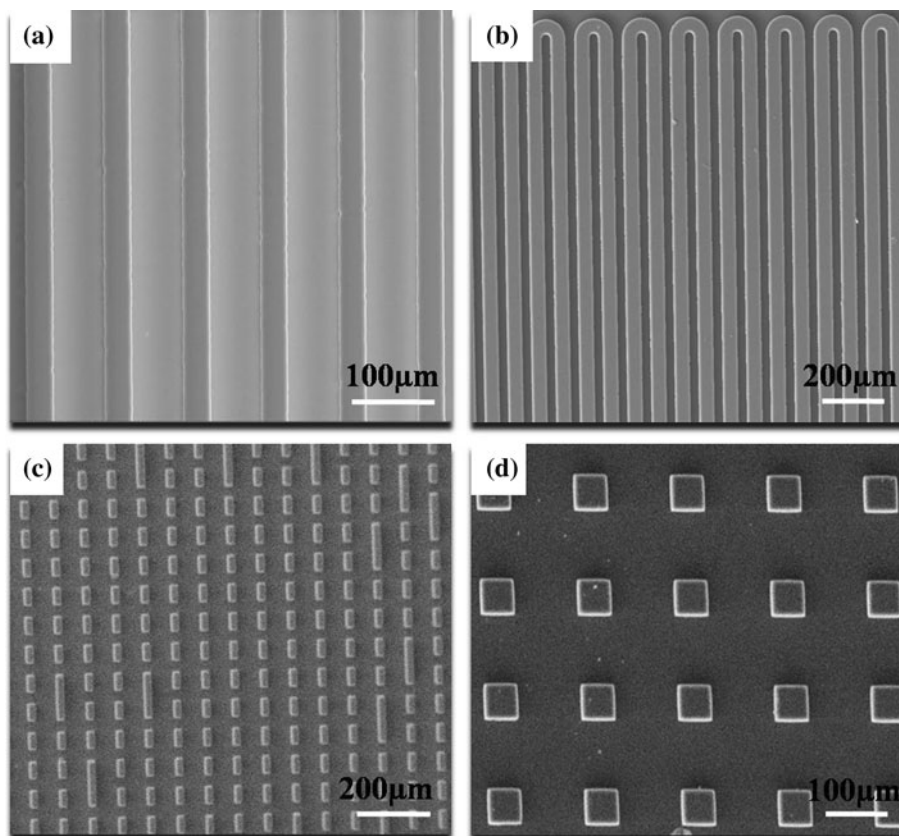


**Scheme 1** Schematic representation of device assembly and subsequent microfluidic growth of ZnO nanostructures inside microchannels

Zn<sup>2+</sup> ions are continuously released in the aqueous DMF solution leading to the precipitation of zinc hydroxide on the Zn surface. Zinc hydroxide embryonic clusters grew into nuclei on the surface which then transformed into zinc oxide.

Figure 1 shows SEM images of PDMS molds with patterned micropillars forming microchannels of

**Fig. 1** SEM images of PDMS molds with micropatterns. **a** Mold 1, **b** Mold 2, **c** Mold 3, and **d** Mold 4



varied profiles. Mold 1 refers to line pattern with pillars of width  $36\ \mu\text{m}$  forming channels of width  $70\ \mu\text{m}$  and height of each pillar is  $45\ \mu\text{m}$ , mold 2 is a serpentine pattern with continuous pillar of width  $60\ \mu\text{m}$  and height of  $45\ \mu\text{m}$  forming continuous channels of width  $30\ \mu\text{m}$ , mold 3 is having rectangular pillar pattern with dimensions as length  $70\ \mu\text{m}$ , width  $20\ \mu\text{m}$ , horizontal distance between two respective rectangles is  $70\ \mu\text{m}$  and vertical distance between the same is  $20\ \mu\text{m}$ , and height  $43\ \mu\text{m}$  and mold 4 is having square pillar pattern with dimensions length  $50\ \mu\text{m}$ , width  $50\ \mu\text{m}$ , horizontal and vertical distance between two respective squares is  $100\ \mu\text{m}$  and height  $20\ \mu\text{m}$ .

Morphological characterization of patterned ZnO nanorod arrays grown on Zn substrates was done by SEM. The SEM images show that vertically aligned ZnO nanorods are grown with high density within geometrically

defined micropatterns. Figure 2a, c, e, g shows the ZnO nanorod arrays grown in microchannels formed by elastomeric Mold 1, Mold 2, Mold 3, Mold 4 and referred as Substrate 1, Substrate 2, Substrate 3 and Substrate 4, respectively. Figure 2b, d, f, h shows magnified images of each pattern with images in inset showing the density of ZnO nanorod arrays on each patterned surface. Figure 3a, b show high resolution SEM images of ZnO nanorods grown in microfluidic channels. These vertically aligned nanorods are observed to have diameter of  $80 \pm 10\ \text{nm}$  and length of  $4 \pm 1\ \mu\text{m}$  at given reaction conditions. These nanostructure arrays grown in different types of microfluidic channels mostly exhibit uniformity in terms of nanorod dimensions and density but in some cases, it is observed that the nanostructures grown at the edges of the channel walls or pillar walls are notably higher than the nanostructures in the centre of the channels. This can be

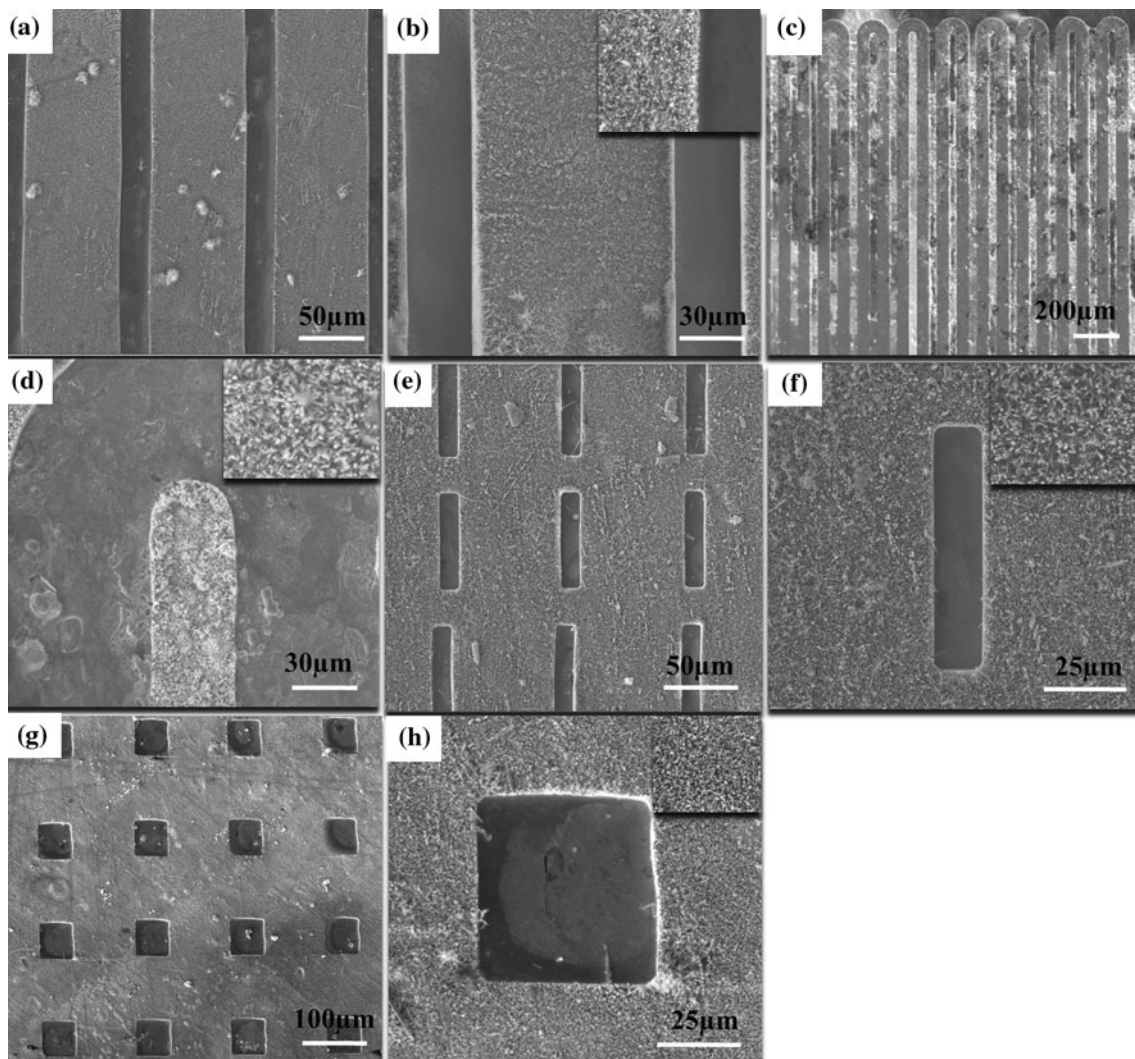
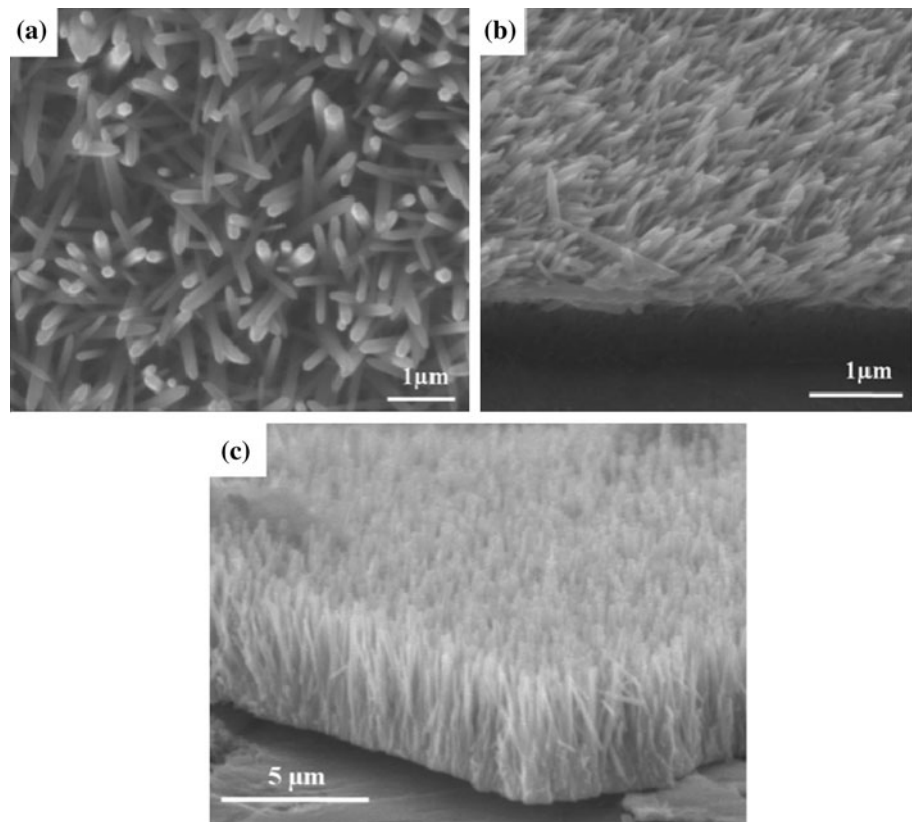


**Fig. 2** SEM images of micropatterned ZnO nanostructures grown in microchannels fabricated by PDMS molds. **a** Substrate 1, **c** Substrate 2, **e** Substrate 3, and **g** Substrate 4; **b**, **d**, **f**, **h** high resolution images of respective substrates with *insets* showing density of nanostructures



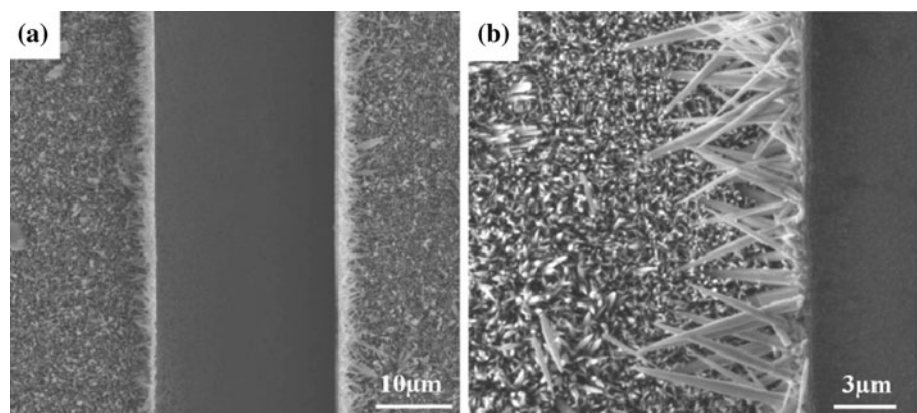
**Fig. 3** High resolution SEM images of ZnO nano structures **a** top view **b** slanted view at 45° angle, and **c** cross section



attributed to the edge effect due to fluid flow in very small channels (Manbachi et al. 2008). Parabolic flow profile of fluids in microchannels results in slow flow of reactant liquids near the channel walls giving more time to them to interact with the active substrate (Zn). Hence, nanostructure growth is accelerated near channel walls making those nanostructures longer as compared to the central nanostructures. Figure 4a, b shows SEM images of ZnO nanostructures grown at the edges of channels. It is observed predominantly in case of ZnO nanostructures grown in straight and serpentine microfluidic channels. Intricate nanostructures can be derived by carefully monitoring reaction conditions, pattern designs and dimensions.

The crystal structure and the orientation of the as grown ZnO nanorods were revealed by the XRD investigation. Figure 5 shows the XRD patterns of the microfluidically prepared ZnO nanorods substrates. All of the diffraction peaks can be indexed to wurtzite structured ZnO (space group  $P63mc$ ;  $a = 0.3249$  nm and  $c = 0.5206$  nm) (JCPDS card no. 35-1451). XRD patterns obtained from all ZnO nanorods substrates show strong peak at  $2\theta = 34.4^\circ$  attributed to the ZnO (002) crystal plane, indicating a preferential orientation of the nanorods along the  $c$ -axes perpendicular to the Zn substrate. The enhanced (002) diffraction peaks are consistent with the SEM images that shows the oriented growth of the ZnO nanorods along the

**Fig. 4** **a, b** SEM images showing ZnO nanostructures grown at the edges of microfluidic channels



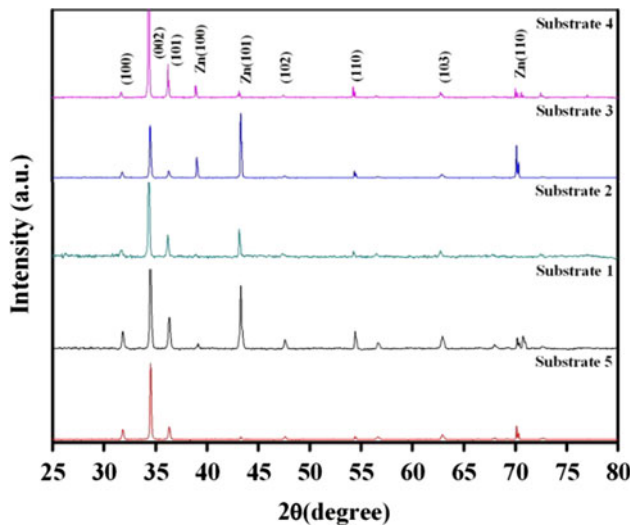


**Fig. 5** XRD patterns of ZnO nanostructures grown in different microchannels. Substrate 5 is ZnO nanostructures grown on Zn wafer without any microconfinement

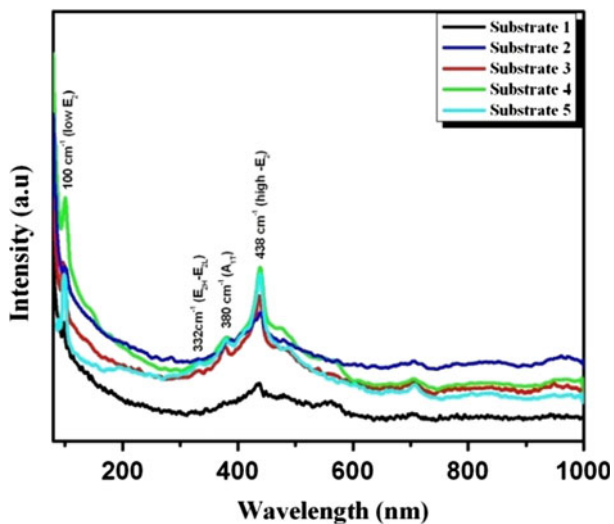
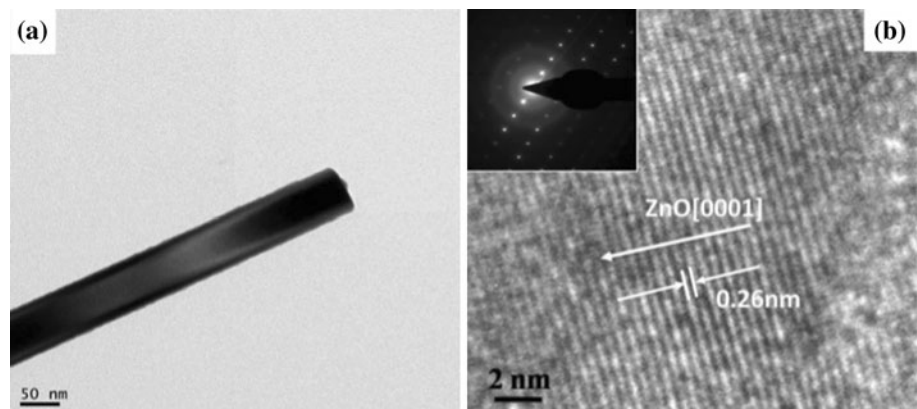


**Fig. 6** Room-temperature Raman spectra of ZnO nanostructures grown in different microchannels

**Fig. 7** **a** TEM image of a single nanorod grown in microchannel. **b** Its HRTEM image with SAED pattern shown in the inset



*c*-axes (Lin et al. 2006). The appearance of the weak (102) and (103) reflections of ZnO was probably caused by the uneven surface of the Zn wafer.

Raman scattering measurements were carried out on as prepared ZnO nanorods substrates to investigate the lattice vibrational properties at room temperature. He–Ne laser ( $\lambda_{\text{exc}} = 632.8 \text{ nm}$ ) is used as the excitation source. Figure 6 shows the Raman spectra of the ZnO nanorods grown in different microfluidic channels. The Raman spectrums of the as grown ZnO nanorods show four prominent peaks at 100, 332, 382, and  $438 \text{ cm}^{-1}$ . The peak at 100 (low- $E_2$ ) and  $438 \text{ cm}^{-1}$  (high  $E_2$ ), a non-polar optical phonons, are clearly visible in all the ZnO nanorods substrates which are common in Wurtzite type of ZnO nanorods (Sieber et al. 2009). Intense and dominant peak is observed at  $438 \text{ cm}^{-1}$  which labeled as  $E_2$  indicates the good crystal quality and is a characteristic of Wurtzite (hexagonal) phase of ZnO. The weak and broad peak at  $332 \text{ cm}^{-1}$  ( $E_{2H}-E_{2L}$ ) is a second order  $E_2$  Raman mode while the peak positioned at  $382 \text{ cm}^{-1}$  can be assigned as  $A_1$  (TO) mode (Liu et al. 2009). The intensity of other peaks is much weaker than  $E_2$  peak suggests that the ZnO nanorods have fewer defects.

The atomic structure of the individual ZnO nanorod is investigated using a high-resolution transmission electron microscopy (HRTEM). Figure 7a, b shows a TEM and HRTEM images of a single nanorod grown within microchannel. The HRTEM investigation shows crystalline ZnO nanorod growth along the ZnO [0001] direction. Also, the diffraction pattern shown in the inset confirms that the nanorods have a single crystalline growth along ZnO [0001] direction.

ZnO is widely studied material for various types of photovoltaic cells. It has high transparency due to the wide band gap and appropriate refractive index ( $n \approx 2$  at 600 nm). Optical and electrical losses are primary factors that influence photovoltaic conversion efficiency. In particular, the optical loss attributed to the reflection loss of the incoming light. By incorporating a novel nano surface textures with multiple internal reflections, low surface

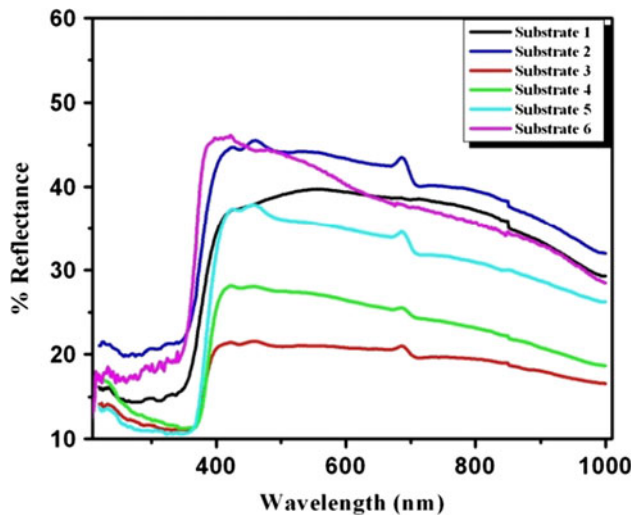


**Fig. 8** Reflectance spectra of ZnO nanostructures grown in microchannels

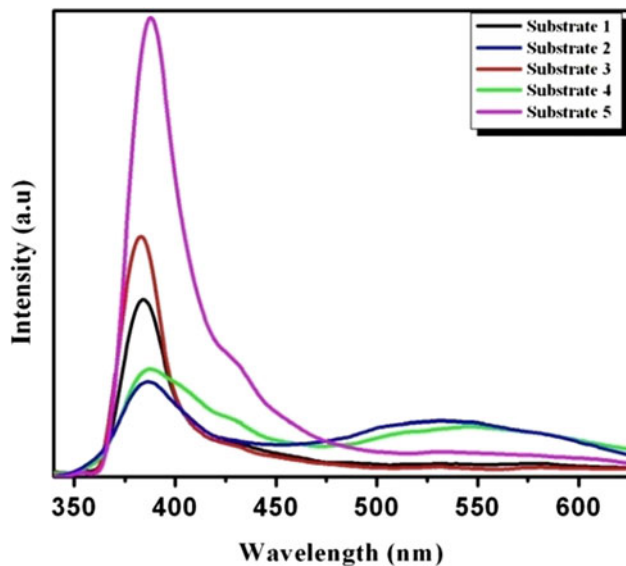


**Fig. 9** RT-PL spectra of hydrothermally prepared patterned and nonpatterned ZnO nanostructures

reflection and high light absorption can be achieved and the efficiency of photovoltaic devices can be significantly enhanced. Micropatterned assembly of ZnO nanostructures resulting in two scale hierarchy can further minimize the reflection loss. In order to verify this logic, we studied the reflectance of all microfluidically grown patterned ZnO nanostructures. The UV–Vis reflectance spectra of all the micropatterned ZnO nanostructures substrates are shown in Fig. 8. Reflectance of unpatterned ZnO nanostructures (Substrate 5) and bare zinc wafer with native thin ZnO layer on its surface (Substrate 6) are taken for reference. Obviously zinc wafer with native thin ZnO layer shows

maximum reflection than all other substrates having ZnO nanorods grown over. ZnO nanorods grown in microfluidic channels with square or rectangular pillar patterns are shown to have minimum reflectance even less than unpatterned substrate having ZnO nanostructures all over its surface and support the logic of reduced reflectance with increased hierarchy. However, nanostructures grown in serpentine and straight line channels show more reflectance than unpatterned surface. This may be because they are having more exposed unstructured area and the less density of the nanorod patterns. It should be possible to minimize reflectance in case channel dimensions are reduced, and subsequently pattern density be increased.

As ZnO is an important material in optoelectronic research (Sieber et al. 2010), the optical quality of ZnO nanorods on Zn substrate is evaluated by the room temperature photoluminescence using 325 nm Xe lamp as the excitation source. Figure 9 shows the RT-PL spectra obtained from the ZnO nanostructures. ZnO nanorods from all patterned substrates exhibit a strong UV emission in the range of 382–387 nm along with the weak violet emission band at 427 nm and broad green emission band in the visible range from 503 to 578 nm. The strong UV emission is the characteristic emission of ZnO and attributed to the radiative recombination of electrons in the conduction band and holes in the valence band. The weak violet emission peak at about 427 nm may be due to the existence of the oxygen depletion interface traps into ZnO film. Zeng et al. (2006), previously reported that, violet emission is attributed to the electronic transition from the defect level to the valence band. Among the six types of defects in ZnO lattice,  $V_o$ ,  $Z_{ni}$  and  $Z_{no}$  are donors, whereas  $V_{Zn}$ ,  $O_i$  and  $O_{Zn}$  are acceptors. Zeng et al. (2010), also proposed a mechanism for the violet emission, if there is excitation of electron to a sub-band of the conduction band, they can first relax to  $Z_{ni}$  state through a non-radiative transition and then move to the valence band. This mechanism suggest that, for violet emission two excitation modes, with  $E_g \leq E_{ex}$  and  $E_{Zni} \leq E_{ex} < E_g$ , are effective. Whereas it is well known that the broad green emission in the visible region is related with defects such as, ionized oxygen vacancies, antisite oxygen, oxygen interstitials, zinc vacancies and surface defects (Gao et al. 2005). UV emission in all ZnO nanorod substrates is stronger than visible emissions which suggest the high crystalline quality of ZnO nanorods.

#### 4 Conclusion

In summary, a robust, inexpensive approach to produce hierarchically structured ZnO nanomaterials is obtained by means of simple microdevice. The resulting micropatterned nanostructures exhibit excellent optical and antireflective

properties. This structural hierarchy can reduce optical loss due to reflectance in photovoltaic cells and subsequently enhance energy conversion efficiency. In order to make this approach more general; films of precursor material can be deposited on desired substrate and nanomaterials that are produced by solution process methods can be assembled hierarchically with ease. It was observed that fluid flow inside microchannels affects growth of nanostructures at the edges; innovative nanostructures can be synthesized inside microfluidic channels by controlling and modulating fluid flow. This method is high throughput and scalable as batch processing is also possible.

**Acknowledgments** We thank Council of Scientific and Industrial Research (CSIR) of India for financially supporting this research.

## References

- Cui Y, Lieber CM (2001) Functional nanoscale electronic devices assembled using silicon nanowire building blocks. *Science* 291:851–853
- Dittrich PS, Heule M, Renaud P, Manz A (2006) On-chip extrusion of lipid vesicles and tubes through micro-sized apertures. *Lab Chip* 6:488–493
- Djurisic AB, Chem X, Leung YH, Ng AMC (2012) ZnO nanostructures: growth, properties and applications. *J Mater Chem* 22:6526–6535
- Duan XF, Huang Y, Cui Y, Wang JF, Lieber CM (2001) Indium phosphide nanowires as building blocks for nanoscale electronic and optoelectronic devices. *Nature* 409:66–69
- Fan HJ, Werner P, Zacharias M (2006) Semiconductor nanowires: from self-organization to patterned growth. *Small* 2:700–717
- Gao X, Li X, Yu W (2005) Flowerlike ZnO nanostructures via hexamethylenetetramine-assisted thermolysis of zinc-ethylene-diamine complex. *J Phys Chem B* 109:1155–1161
- Govender K, Boyle DS, O'Brien P, Binks D, West D, Coleman D (2002) Room-temperature lasing observed from ZnO nanocolumns grown by aqueous solution deposition. *Adv Mater* 14:1221–1224
- Greyson EC, Babayan Y, Odom TW (2004) Directed growth of ordered arrays of small-diameter ZnO nanowires. *Adv Mater* 16:1348–1352
- Han X, Zhou X, Jiang Y, Xie Z (2012) The preparation of spiral, ZnO nanostructures by top-down wet-chemical etching and their related properties. *J Mater Chem* 22:10924–10928
- Huang MH, Mao S, Feick H, Yan H, Wu Y, Kind H, Weber E, Russo R, Yang P (2001) Room-temperature ultraviolet nanowire nanolasers. *Science* 292:1897–1899
- Jung MH, Lee H (2011) Selective patterning of ZnO nanorods on silicon substrates using nanoimprint lithography. *Nanoscale Res Lett* 6:159
- Kang HW, Yeo J, Hwang JO, Hong S, Lee P, Han SY, Lee JH, Rho YS, Kim SO, Ko SH, Sung HJ (2011) Simple ZnO nanowires patterned growth by microcontact printing for high performance field emission device. *J Phys Chem C* 115:11435–11441
- Kenis PJA, Ismagilov RF, Takayama S, Whitesides GM, Li S, White HS (2000) Fabrication inside microchannels using fluid flow. *Acc Chem Res* 33:841–847
- Kim DS, Ji R, Fan HJ, Bertram F, Scholz R, Dadgar A, Nielsch K, Krost A, Christen J, Gosele U, Zacharias M (2007) Laser-interference lithography tailored for highly symmetrically arranged ZnO nanowire arrays. *Small* 3:76–80
- Kim J, Lib Z, Park I (2011) Direct synthesis and integration of functional nanostructures in microfluidic devices. *Lab Chip* 11:1946–1951
- Law M, Greene LE, Johnson JC, Saykally R, Yang P (2005) Nanowire dye-sensitized solar cells. *Nat Mater* 4:455–459
- Lee SH, Lee HJ, Oh D, Lee SW, Goto H, Buckmaster R, Yasukawa T, Matsue T, Hong SK, Ko HC et al (2006) Control of the ZnO nanowires nucleation site using microfluidic channels. *J Phys Chem B* 110:3856–3859
- Lin YR, Yang SS, Tsai SY, Hsu HC, Wu ST, Chen IC (2006) Visible photoluminescence of ultrathin ZnO nanowire at room temperature. *Cryst Growth Des* 6:1951–1955
- Liu H, Piret G, Sieber B, Laureyns J, Roussel P, Xu W, Boukherroub R, Szunerits S (2009) Electrochemical impedance spectroscopy of ZnO nanostructures. *Electrochem Commun* 11:945–949
- Manbachi A, Shrivastava S, Cioffi M, Chung BG, Moretti M, Demirci U, Yliperttula M, Khademhosseini A (2008) Microcirculation within grooved substrates regulates cell positioning and cell docking inside microfluidic channels. *Lab Chip* 8:747–754
- Menard E, Rogers JA (2007) Stamping techniques for micro- and nanofabrication. In: Bhushan B (ed) *Springer handbook of nanotechnology*. Springer, Berlin, pp 279–298
- Ng HT, Han J, Yamada T, Nguyen P, Chen YP, Meyyappan M (2004) Single crystal nanowire vertical surround-gate field-effect transistor. *Nano Lett* 4:1247–1252
- Ong WL, Low QX, Huang W, Van Kan JA, Ho GW (2012) Patterned growth of vertically-aligned ZnO nanorods on a flexible platform for feasible transparent and conformable electronics applications. *J Mater Chem* 22:8518–8524
- Park WI, Yi GC (2004) Electroluminescence in n-ZnO nanorod arrays vertically grown on p-GaN. *Adv Mater* 16:87–90
- Qin D, Xia Y, Whitesides GM (2010) Soft lithography for micro- and nanoscale patterning. *Nat Protoc* 5:491–502
- Qu L, Vaia RA, Dai L (2011) Multilevel, multicomponent microarchitectures of vertically-aligned carbon nanotubes for diverse applications. *ACS Nano* 5:994–1002
- Sieber B, Liu H, Piret G, Laureyns J, Roussel P, Gelloz B, Szunerits S, Boukherroub R (2009) Synthesis and luminescence properties of (N-doped) ZnO nanostructures from a dimethylformamide aqueous solution. *J Phys Chem C* 113:13643–13650
- Sieber B, Addad A, Szunerits S, Boukherroub R (2010) Stacking faults-induced quenching of the UV luminescence in ZnO. *J Phys Chem Lett* 1:3033–3038
- Thangawng L, Howell PB, Richards JJ, Erickson JS, Ligler FS (2009) A simple sheath-flow microfluidic device for micro/nanomanufacturing: fabrication of hydrodynamically shaped polymer fibers. *Lab Chip* 9:3126–3130
- Wang ZL, Song JH (2006) Piezoelectric nanogenerators based on zinc oxide nanowire arrays. *Science* 312:242–246
- Wang X, Summers CJ, Wang ZL (2004) Large-scale hexagonal-patterned growth of aligned ZnO nanorods for nano-optoelectronics and nanosensor arrays. *Nano Lett* 4:423–426
- Wang WZ, Zeng BQ, Yang J, Poudel B, Huang JY, Naughton MJ, Ren ZF (2006a) Aligned ultralong ZnO nanobelts and their enhanced field emission. *Adv Mater* 18:3275–3278
- Wang J, Bunimovich YL, Sui G, Sawas S, Wang J, Guo Y, Heath JR, Tseng HR (2006) Electrochemical fabrication of conducting polymer nanowires in an integrated microfluidic system. *Chem Commun* 3075–3077
- Wang H, Wong ASW, Ho GW (2007) Facile solution route to vertically aligned, selective growth of ZnO nanostructure arrays. *Langmuir* 23:11960–11963
- Wang Y, Li X, Lu G, Quan X, Chen G (2008) Highly oriented 1-D ZnO nanorod arrays on zinc foil: direct growth from substrate, optical properties and photocatalytic activities. *J Phys Chem C* 112:7332–7336



- Xu S, Wang ZL (2011) One-dimensional ZnO nanostructures: solution growth and functional properties. *Nano Res* 4:1013–1098
- Yang PD, Yan RX, Fardy M (2010) Semiconductor nanowire: what's next? *Nano Lett* 10:1529–1536
- Yen BKH, Gunther A, Schmidt MA, Jensen KF, Bawendi MGA (2005) A microfabricated gas–liquid segmented flow reactor for high-temperature synthesis: the case of CdSe quantum dots. *Angew Chem Int Ed* 44:5447–5451
- Zeng H, Cai W, Hu J, Duan G, Liu P (2006) Violet photoluminescence from shell layer of Zn/ZnO core-shell nanoparticles induced by laser ablation. *Appl Phys Lett* 88:171910–171913
- Zeng H, Xu X, Bando Y, Gautam UK, Zhai T, Fang X, Liu B, Golberg D (2009) Template deformation-tailored ZnO nanorod/nanowire arrays: full growth control and optimization of field-emission. *Adv Funct Mat* 19:3165–3172
- Zeng H, Duan G, Li Y, Yang S, Xu X, Cai W (2010) Blue luminescence of ZnO nanoparticles based on non-equilibrium processes: defect origins and emission controls. *Adv Funct Mat* 20:561–572